UNITÉ DE RECHERCHE
INRIA-SOPHIA ANTIPOLIS

Rapports de Recherche

N°1894

Programme 4

Robotique, Image et Vision

ON DETERMINING THE FUNDAMENTAL MATRIX: ANALYSIS OF DIFFERENT METHODS AND EXPERIMENTAL RESULTS

Quang-Tuan Luong
Rachid Deriche
Olivier Faugeras
Theo Papadopoulo

Avril 1993

Institut National
de Recherche
en Informatique
et en Automatique

2004 route des Lucioles
B.P. 93
06902 Sophia-Antipolis
France

On Determining the Fundamental Matrix: Analysis of Different Methods and Experimental Results

Détermination de la matrice fondamentale: Analyse de différentes méthodes et résultats expérimentaux

Quang-Tuan Luong Rachid Deriche Olivier Faugeras
Théodore Papadopoulo

INRIA Sophia Antipolis
BP 93 - Sophia-Antipolis Cedex
France

Programme 4: Robotique, Image et Vision

Abstract

The *Fundamental matrix* is a key concept when working with uncalibrated images and multiple viewpoints. It contains all the available geometric information and enables to recover the epipolar geometry from uncalibrated perspective views. This paper addresses the important problem of its robust determination given a number of image point correspondences. We first define precisely this matrix, and show clearly how it is related to the epipolar geometry and to the *Essential matrix* introduced earlier by Longuet-Higgins. In particular, we show that this matrix, defined up to a scale factor, must be of rank two. Different parametrizations for this matrix are then proposed to take into account these important constraints and linear and non-linear criteria for its estimation are also considered. We then clearly show that the linear criterion is unable to express the rank and normalization constraints. Using the linear criterion leads definitely to the worst result in the determination of the *Fundamental matrix*. Several examples on real images clearly illustrate and validate this important negative result. To overcome the major weaknesses of the linear criterion, different non-linear criteria are proposed and analyzed in great detail. Extensive experimental work has been performed in order to compare the different methods using a large number of noisy synthetic data and real images. In particular, a statistical method based on variation of camera displacements is used to evaluate the stability and convergence properties of each method.

Keywords:
Motion Analysis, Calibration, Projective Geometry.

Résumé

La *matrice fondamentale* est un concept-clé pour toutes les questions touchant à l'emploi d'images non calibrées prises de points de vue multiples. Elle contient toute l'information géométrique disponible et permet d'obtenir la géométrie épipolaire à partir de deux vues perspectives non calibrées. Ce rapport est à propos du problème important de sa détermination robuste à partir d'un certain nombre de correspondances ponctuelles. Nous commençons par définir précisément cette matrice, et par mettre en évidence ses relations avec la géométrie épipolaire et la *matrice essentielle*, introduite précédemment par Longuet-Higgins. En particulier, nous montrons que cette matrice, définie à un facteur d'échelle, doit être de rang deux. Les techniques linéaires d'estimation de la matrice essentielle admettent une extension naturelle qui permet d'effectuer le calcul direct de la matrice fondamentale à partir d'appariements de points, au moyen d'un critère qui est linéaire. Nous montrons que cette méthode souffre de deux défauts, liés à l'absence de contrainte sur le rang de la matrice recherchée, et à l'absence de normalisation du critère, qui entraînent des erreurs importantes dans l'estimation de la matrice fondamentale et des épipoles. Cette analyse est validée par plusieurs exemples réels. Afin de surmonter ces difficultés, plusieurs nouveaux critères non-linéaires, dont

nous donnons des interprétations en termes de distances, sont ensuite proposés, puis plusieurs paramétrisations sont introduites pour rendre compte des contraintes auxquelles doit satisfaire la matrice fondamentale. Un travail expérimental exhaustif est réalisé à l'aide de nombreuses données synthétiques et d'images réelles. En particulier, une méthode statistique fondée sur la variation des déplacements de la caméra est utilisée pour évaluer la stabilité et les propriétés de convergence des différentes méthodes.

Mots-clé:
Analyse du mouvement, calibration, géométrie projective

1 Introduction

Inferring three-dimensional information from images taken from different viewpoints is a central problem in computer vision. However, as the measured data in images are just pixel coordinates, there are only two approaches that can be used in order to perform this task:

The first one is to establish a model which relates pixel coordinates to 3D coordinates, and to compute the parameters of such a model. This is done by camera calibration [21] [5], which typically computes the projection matrices $\mathbf{P}$, which relates the image coordinates to a world reference frame. However, it is not always possible to assume that cameras can be calibrated off-line, particularly when using active vision systems.

Thus a second approach is emerging, which consists in using projective invariants [16], whose non-metric nature allows to use uncalibrated cameras. Recent work [8] [3] [15] [6] has shown that it is possible to recover the projective structure of a scene from point correspondences only, without the need for camera calibration. It is even possible to use these projective invariants to compute the camera calibration [4] [14]. These approaches use only geometric information which relates the different viewpoints. This information is entirely contained in the *Fundamental matrix*, thus it is very important to develop precise techniques to compute it.

In spite of the fact that there has been some confusion between the fundamental matrix and Longuet-Higgins essential matrix, it is now known that the fundamental matrix can be computed from pixel coordinates of corresponding points. Line correspondences are not sufficient with two views. Another approach is to use linear filters tuned to a range of orientations and scales. Jones and Malik [9] have shown that it is also possible in this framework to recover the location of epipolar lines. The computation technique used by most of the authors [6] [18] [20] is just a linear one, which generalizes the eight-point algorithm of Longuet-Higgins[13]. After a first part where we clarify the concept of Fundamental matrix, we show that this computation technique suffers from two majors intrinsic drawbacks. Analyzing these drawbacks enables us to introduce a new, non-linear computation technique, based on criteria that have a nice interpretation in terms of distances. We then show, using both large sets of simulations and real data, that our non-linear computation techniques provide significant improvement in the accuracy of the Fundamental matrix determination.

2 The Fundamental Matrix

2.1 The projective model

The camera model which is most widely used is the pinhole: the camera is supposed to perform a perfect perspective transformation of 3D space on a retinal plane. In the general case, we must also account for a change of world coordinates, as well as for a change of retinal coordinates, so that a generalization of the previous assumption is that the camera performs a *projective linear transformation*, rather than a mere perspective transformation. The *pixel coordinates* u and v are the only information we

have if the camera is not calibrated:

$$\mathbf{q} = \begin{bmatrix} su \\ sv \\ s \end{bmatrix} = \mathbf{A} \begin{bmatrix} 1 & 0 & 0 & 0 \\ 0 & 1 & 0 & 0 \\ 0 & 0 & 1 & 0 \end{bmatrix} \mathbf{G} \begin{bmatrix} X \\ Y \\ Z \\ 1 \end{bmatrix} \equiv \mathbf{PM} \tag{1}$$

where X, Y, Z are world coordinates, $\mathbf{A}$ is a 3×3 transformation matrix accounting for camera sampling and optical characteristics and $\mathbf{G}$ is a 4×4 displacement matrix accounting for camera position and orientation. If the camera is calibrated, then $\mathbf{A}$ is known and it is possible to use *normalized coordinates* $\mathbf{m} = \mathbf{A}^{-1}\mathbf{q}$, which have a direct 3D interpretation.

2.2 The epipolar geometry and the Fundamental matrix

The epipolar geometry is the basic constraint which arises from the existence of two viewpoints. Let a camera take two images by linear projection from two different locations, as shown in figure 1. Let $\mathbf{C}$ be the optical center of the camera when the first image is obtained, and let $\mathbf{C}'$ be the optical center for the second image. The line $\langle \mathbf{C}, \mathbf{C}' \rangle$ projects to a point $\mathbf{e}$ in the first image $\mathcal{R}_1$, and to a point $\mathbf{e}'$ in the second image $\mathcal{R}_2$. The points $\mathbf{e}$, $\mathbf{e}'$ are the epipoles. The lines through $\mathbf{e}$ in the first image and the lines through $\mathbf{e}'$ in the second image are the epipolar lines. The epipolar constraint is well-known in stereovision: for each point $\mathbf{m}$ in the first retina, its corresponding point $\mathbf{m}'$ lies on its epipolar line $\mathbf{l}'_m$.

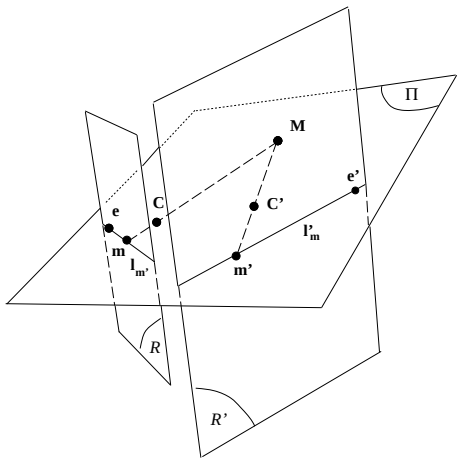

Figure 1: The epipolar geometry

Let us now use retinal coordinates. The relationship between a point $\mathbf{q}$ and its corresponding epipolar line $\mathbf{l}'_q$ is projective linear, because the relations between $\mathbf{q}$ and $\langle \mathbf{C}, \mathbf{M} \rangle$, and $\mathbf{q}$ and $\langle \mathbf{C}, \mathbf{M} \rangle$ and its projection $\mathbf{l}'_q$ are both projective linear. We call the 3×3 matrix $\mathbf{F}$ which describes this correspondence the *fundamental matrix*. The importance of the fundamental matrix has been neglected in the literature, as almost all the work on motion has been done under the assumption that intrinsic parameters

are known. In that case, the fundamental matrix reduces to an essential matrix. But if one wants to proceed only from image measurements, the fundamental matrix is the key concept, as it contains the all the geometrical information relating two different images.

2.3 Relation with Longuet-Higgins equation

The Longuet-Higgins equation [13], applies when using normalized coordinates, and thus calibrated cameras. If the motion between the two positions of the cameras are given by the rotation matrix $\mathbf{R}$ and the translation matrix $\mathbf{t}$, and if $\mathbf{m}$ and $\mathbf{m}'$ are corresponding points, then the coplanarity constraint relating $\mathbf{Cm}'$, $\mathbf{t}$, and $\mathbf{Cm}$ is written as:

$$\mathbf{m}' \cdot (\mathbf{t} \times \mathbf{Rm}) \equiv \mathbf{m}'^T \mathbf{Em} = 0 \tag{2}$$

The matrix $\mathbf{E}$, which is the product of an orthogonal matrix and an antisymmetric matrix is called an essential matrix. Because of the depth/speed ambiguity, $\mathbf{E}$ depends on five parameters only.

Let us now express the epipolar constraint using the fundamental matrix, in the case of uncalibrated cameras. For a given point $\mathbf{q}$ in the first image, the projective representation $\mathbf{l}'_q$ of its the epipolar line in the second image is given by

$$\mathbf{l}'_q = \mathbf{Fq}$$

Since the point $\mathbf{q}'$ corresponding to $\mathbf{q}$ belongs to the line $\mathbf{l}'_q$ by definition, it follows that

$$\mathbf{q}'^T \mathbf{Fq} = 0 \tag{3}$$

It can be seen that the two equations (2) and (3) are equivalent, and that we have the relation:

$$\mathbf{F} = \mathbf{A}^{-1T} \mathbf{E} \mathbf{A}^{-1}$$

Unlike the essential matrix, which is characterized by the two constraints found by Huang and Faugeras [7] which are the nullity of the determinant and the equality of the two non-zero singular values, the only property of the fundamental matrix is that it is of rank two. As it is also defined only up to a scale factor, the number of independent coefficients of $\mathbf{F}$ is seven.

2.4 Relation with the epipolar transformation

The epipolar transformation is a homography between the epipolar lines in the first image and the epipolar lines in the second image, defined as follows. Let Π be any plane containing $\langle \mathbf{C}, \mathbf{C}' \rangle$. Then Π projects to an epipolar line l in the first image and to an epipolar line l' in the second image. The correspondences $\Pi \overline{\wedge} l$ and $\Pi \overline{\wedge} l'$ are homographies between the two pencils of epipolar lines and the pencil of planes containing $\langle \mathbf{C}, \mathbf{C}' \rangle$. It follows that the correspondance $l \overline{\wedge} l'$ is a homography. In the practical case where epipoles are at finite distance, the epipolar transformation is characterized by

the *affine* coordinates of the epipoles $\mathbf{e}$ and $\mathbf{e}'$ and by the coefficients of the homography between the two pencils of epipolar lines, *each line being parameterized by its direction*:

$$\tau \mapsto \tau' = \frac{a\tau + b}{c\tau + d} \tag{4}$$

where

$$\tau = \frac{q_2 - e_2}{q_1 - e_1} \qquad \tau' = \frac{q_2' - e_2'}{q_1' - e_1'} \tag{5}$$

and $\mathbf{q} \leftrightarrow \mathbf{q}'$, is a pair of corresponding points. It follows that the epipolar transformation, like the fundamental matrix depends on seven independent parameters.

On identifying the equation (3) with the constraint on epipolar lines obtained by making the substitutions (5) in (4), expressions are obtained for the coefficients of $\mathbf{F}$ in terms of the parameters describing the epipoles and the homography:

$$\begin{aligned}
F_{11} &= be_3e_3' \\
F_{12} &= ae_3e_3' \\
F_{13} &= -ae_2e_3' - be_1e_3' \\
F_{21} &= -de_3'e_3 \\
F_{22} &= -ce_3'e_3 \\
F_{23} &= ce_3'e_2 + de_3'e_1 \\
F_{31} &= de_2'e_3 - be_3e_1' \\
F_{32} &= ce_2'e_3 - ae_3e_1' \\
F_{33} &= -ce_2'e_2 - de_2'e_1 + ae_2e_1' + be_1e_1'
\end{aligned} \tag{6}$$

From these relations, it is easy to see that $\mathbf{F}$ is defined only up to a scale factor. Let $\mathbf{c}_1$, $\mathbf{c}_2$, $\mathbf{c}_3$ be the columns of $\mathbf{F}$. It follows from (6) that $e_1\mathbf{c}_1 + e_2\mathbf{c}_2 + e_3\mathbf{c}_3 = 0$. The rank of $\mathbf{F}$ is thus at most two. The equations (6), yield the epipolar transformation as a function of the fundamental matrix:

$$\begin{aligned}
a &= F_{12} \\
b &= F_{11} \\
c &= -F_{22} \\
d &= -F_{21} \\
e_1 &= \frac{F_{23}F_{12} - F_{22}F_{13}}{F_{22}F_{11} - F_{21}F_{12}}e_3 \\
e_2 &= \frac{F_{13}F_{21} - F_{11}F_{23}}{F_{22}F_{11} - F_{21}F_{12}}e_3 \\
e_1' &= \frac{F_{32}F_{21} - F_{22}F_{31}}{F_{22}F_{11} - F_{21}F_{12}}e_3' \\
e_2' &= \frac{F_{31}F_{12} - F_{11}F_{32}}{F_{22}F_{11} - F_{21}F_{12}}e_3'
\end{aligned} \tag{7}$$

The determinant $ad - bc$ of the homography is $F_{22}F_{11} - F_{21}F_{12}$. In the case of finite epipoles, it is not null. The interpretation of equations (7) is simple: the coordinates

of $\mathbf{e}$ (resp. $\mathbf{e}'$) are the vectors of the kernel of $\mathbf{F}$ (resp. $\mathbf{F}^T$). Writing τ' as a function of τ from the relation $\mathbf{y}'_\infty \mathbf{F} \mathbf{y}_\infty = 0$ which arises from the correspondence of the points at infinity $\mathbf{y}_\infty = (1, \tau, 0)^T$ et $\mathbf{y}'_\infty = (1, \tau', 0)^T$, of corresponding lines, we obtain the homographic relation.

3 The linear criterion

3.1 The eight point algorithm

Equation (3) can be written:

$$\mathbf{U}^T \mathbf{f} = 0 \tag{8}$$

where:

$$\begin{aligned} \mathbf{U} &= [uu', vu', u', uv', vv', v', u, v, 1] \\ \mathbf{f} &= [F_{11}, F_{12}, F_{13}, F_{21}, F_{22}, F_{23}, F_{31}, F_{32}, F_{33}] \end{aligned}$$

Equation (8) is linear and homogeneous in the 9 unknown coefficients of matrix $\mathbf{F}$. Thus we know that if we are given 8 matches we will be able, in general, to determine a unique solution for $\mathbf{F}$, defined up to a scale factor. This approach, known as the eight point algorithm, was introduced by Longuet-Higgins [13] and has been extensively studied in the literature [12] [22] [2] [23] [11], for the computation of the *Essential matrix*. It has proven to be very sensitive to noise. Our contribution is to study it in the more general framework of *Fundamental matrix* computation. Some recent work has indeed pointed out that it is also relevant for the purpose of working from uncalibrated cameras [18], [4] [6]. In this framework, we obtain new results about the accuracy of this criterion, which will enable us to present a more robust approach.

3.2 Implementations

In practice, we are given much more than 8 matches and we use a least-squares method to solve:

$$\min_{\mathbf{F}} \sum_i (\mathbf{q}_i'^T \mathbf{F} \mathbf{q}_i)^2 \tag{9}$$

which can be rewritten as:

$$\min_{\mathbf{f}} \|\tilde{\mathbf{U}} \mathbf{f}\|^2$$

where:

$$\tilde{\mathbf{U}} = \begin{bmatrix} \mathbf{U}_1^T \\ \vdots \\ \mathbf{U}_n^T \end{bmatrix}$$

We have tried different implementations. The first one (**M-C**) uses a closed-form solution via the linear equations. One of the coefficients of $\mathbf{F}$ must be set to 1. The second one solves the classical problem:

$$\min_{\mathbf{f}} \|\tilde{\mathbf{U}} \mathbf{f}\| \quad \text{with} \quad \|\mathbf{f}\| = 1 \tag{10}$$

The solution is the eigenvector associated to the smallest eigenvalue of $\tilde{\mathbf{U}}^T\tilde{\mathbf{U}}$, which we compute directly (**DIAG**), or using a singular value decomposition (**SVD**). The advantage of this second approach is that all the coefficients of $\mathbf{F}$ play the same role. We have also tried to normalize the projective coordinates to use the Kanatani N-vectors representation [10] (**DIAG-N**).

The advantage of the linear criterion is that it leads to a non-iterative computation method, however, we have found that it is quite sensitive to noise, even with numerous data points. The two main reasons for this are:

- The constraint $\det(\mathbf{F}) = 0$ is not satisfied, which causes inconsistencies of the epipolar geometry near the epipoles.
- The criterion is not normalized, which causes a bias in the localization of the epipoles.

3.3 The linear criterion cannot express the rank constraint

Let l' be an epipolar line in the second image, computed from a fundamental matrix $\mathbf{F}$ that was obtained by the linear criterion, and from the point $\mathbf{m} = (u, v, 1)^T$ of the first image. We can express $\mathbf{m}$ using the epipole in the first image, and the horizontal and vertical distances from this epipole, x and y. A projective representation for l' is:

$$\mathbf{l}' = \mathbf{F}\mathbf{m} = \mathbf{F}\begin{pmatrix} e_1 - x \\ e_2 - y \\ 1 \end{pmatrix} = \mathbf{F}\mathbf{e} - \underbrace{\mathbf{F}\begin{pmatrix} x \\ y \\ 0 \end{pmatrix}}_{\mathbf{l}_1} \tag{11}$$

If $\det(\mathbf{F}) = 0$, the epipole $\mathbf{e}$ satisfies exactly $\mathbf{F}\mathbf{e} = 0$, thus the last expression simplifies to $\mathbf{l}_1$. It is easy to see that it defines an epipolar line which goes through the epipole $\mathbf{e}'$ in the second image. If the determinant is not exactly zero, we see that $\mathbf{l}'$ is the sum of a constant vector $\mathbf{r} = \mathbf{F}\mathbf{e}$ which should be zero but is not, and of the vector $\mathbf{l}_1$, whose norm is bounded by $\sqrt{x^2 + y^2}\|\mathbf{F}\|$. We can conclude that when $(x, y) \to (0, 0)$ ($\mathbf{m} \to \mathbf{e}$), the epipolar line of $\mathbf{m}$ in the second image converges towards a fixed line represented by $\mathbf{r}$, which is inconsistent with the notion of epipolar geometry. We can also see that the smaller $\sqrt{x^2 + y^2}$ is (ie the closer $\mathbf{m}$ is to the epipole), the bigger will be the error on its associated epipolar line.

We can make these remarks more precise by introducing an Euclidean distance. If the coordinates of the point $\mathbf{p}$ are (x_0, y_0), and if $l_1 x + l_2 y + l_3 = 0$ is the equation of the line l, then the distance of the point $\mathbf{p}$ to the line l is:

$$d(\mathbf{p}, l) = \frac{|l_1 x_0 + l_2 y_0 + l_3|}{\sqrt{l_1^2 + l_2^2}} \tag{12}$$

The distance of the epipolar line $l'(\mathbf{m})$ given by (11) to the epipole $\mathbf{e}' = (e'_1, e'_2, 1)^T$ is thus:

$$d(\mathbf{e}', l') = \frac{|r_1 e'_1 + r_2 e'_2 + r_3 - (F_{11}e'_1 + F_{21}e'_2 + 1)x - (F_{12}e'_1 + F_{22}e'_2 + 1)y|}{\sqrt{(r_1 - F_{11}x - F_{12}y)^2 + (r_2 - F_{21}x - F_{22}y)}} \tag{13}$$

It is clear that when $(x, y) \to (0, 0)$, $d(\mathbf{e}', l') \to \frac{r_1 e'_1 + r_2 e'_2 + r_3}{\sqrt{r_1^2 + r_2^2}}$, which is a generally a big value.

We now give a real example to illustrate these remarks. The images and the matched points are the ones of figure 8. The values of the residual vectors $\mathbf{r} = \mathbf{F}\mathbf{e}$ and $\mathbf{r}' = \mathbf{F}^T\mathbf{e}'$ are:

$$\mathbf{r} = (.0000197, .0000274, .630\ 10^{-7})^T \quad \mathbf{r}' = (.0000203, .0000236, .152\ 10^{-6})^T$$

They seem very low, as $\|r\| = .000033$, however this is to be compared with the residuals found by the non-linear criterions presented later, whose typical values are $\|r\| = .2\ 10^{-7}$. The figure 2 shows a plot of the error function (13), versus the distances x and y. Units are pixels. We can see that there is a very sharp peak near the point $(x, y) = 0$, which represents the epipole $\mathbf{e}$, and that the error decreases and converges to a small value. We can conclude that *if the epipole is in the image, the epipolar geometry described by the fundamental matrix obtained from the linear criterion will be inaccurate.*

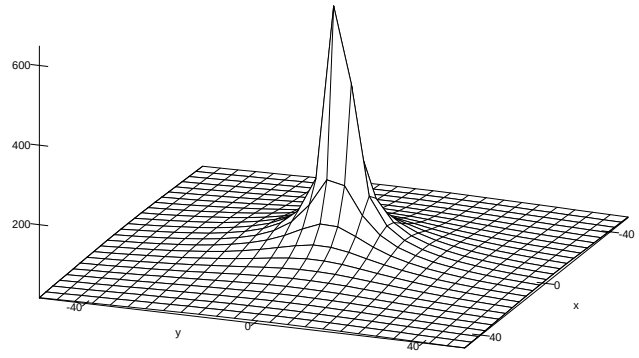

Figure 2: Distances of epipolar lines to the epipole, linear criterion

This problem can be observed directly in the images shown in the experimental part, in figure 10 for the intersection of epipolar lines, and in figure 11, for the inconsistency of epipolar geometry near the epipoles.

3.4 The linear criterion suffers from lack of normalization

Let us now give a geometrical interpretation of the criterion (9). Using again (12), the Euclidean distance of the point $\mathbf{q}'$ of the second image to the epipolar line $\mathbf{l}' =$

$(l'_1, l'_2, l'_3)^T = \mathbf{F}\mathbf{q}$ of the corresponding point $\mathbf{q}$ of the first image is:

$$d(\mathbf{q}', \mathbf{l}') = \frac{|\mathbf{q}'^T \mathbf{l}'|}{\sqrt{(l'_1)^2 + (l'_2)^2}} \tag{14}$$

We note that this expression is always valid as the normalizing term $k = \sqrt{(l'_1)^2 + (l'_2)^2}$ is null only in the degenerate cases where the epipolar line is at infinity. The criterion (9) can be written:

$$\sum_i k_i^2 d^2(\mathbf{q}'_i, \mathbf{l}'_i) \tag{15}$$

This interpretation shows that a geometrically significant quantity in the linear criterion is the distance of a point to the epipolar line of its corresponding point. This quantity is weighted by the coefficients k, defined above.

To see why it can introduce a bias, let us first consider the case where the displacement is a pure translation. The fundamental matrix is antisymmetric and has the form:

$$\begin{bmatrix} 0 & 1 & -y \\ -1 & 0 & x \\ y & -x & 0 \end{bmatrix}$$

where $(x, y, 1)^T$ are the coordinates of the epipoles, which are the same in the two images. If $(u_i, v_i, 1)^T$ are the coordinates of the point $\mathbf{q}_i$ in the first image, then the normalizing factor is $k_i^2 = \lambda^2((y - v_i)^2 + (x - u_i)^2)$, where λ is a constant. When minimizing the criterion (15), we will minimize both k_i and $d^2(\mathbf{q}'_i, \mathbf{l}'_i)$. But minimizing k_i is the same than privileging the fundamental matrices which yield epipoles near the image. Experimental results show that it is indeed the case. A first example is given by the images already used: we can see that the epipoles found by the linear criterion, which are at position:

$$\mathbf{e} = (403.90, 603.24, 1)^T \quad \mathbf{e}' = (408.38, 524.63, 1)^T$$

are nearer than the ones found by the non-linear criterion presented latter, as the epipolar lines obtained from the non-linear criterion are almost parallel in the images, as can be seen in figure 8. A second example is given by table 1.

In the general case, the normalizing factor is:

$$k_i = (a(y - v_i) + b(x - u_i))^2 + (c(y - v_i) + d(x - u_i))^2$$

To see simply its effect on the minimization, let suppose that the coefficients of the homography are fixed. By computing the partial derivatives $\frac{\partial k_i}{\partial x}$ and $\frac{\partial k_i}{\partial y}$, it is easy to see that the minimum is obtained for $x = u_i$ and $y = v_i$. Thus the previous observations apply too. We can conclude that *the linear criterion shifts epipoles towards the image center.*

We can notice that the situation is particularly bad with the linear criterion, due to the combination of our two observations: whereas the closer the epipoles are to the images, the less accurate will be the epipolar geometry, the epipoles tend to be shifted towards the image center.

Table 1: An example to illustrate the behaviour of the linear criterion when the displacement is a translation

$\mathbf{R} = \mathbf{I} \quad \mathbf{t} = [0\ 100\ 100]$				
image noise (pixel)	coordinates of the epipoles			
	e_x	e_y	e'_x	e'_y
0	246.09	1199.34	246.09	1199.34
0.1	246.09	1193.49	245.06	1193.68
0.5	239.63	1027.16	253.20	1027.23
1.0	237.22	758.55	263.33	767.01
2.0	242.54	544.70	263.01	568.16

4 Non-Linear criteria

4.1 The distance to epipolar lines

We now introduce a first non-linear approach, based on the geometric interpretation of criterion (9) given in 3.4. The first idea is to use a non-linear criterion, minimizing:

$$\sum_i d^2(\mathbf{q}'_i, \mathbf{F}\mathbf{q}_i)$$

However, unlike the case of the linear criterion, the two images do not play a symmetric role, as the criterion determines only the epipolar lines in the second image, and should not be used to obtain the epipole in the first image. We would have to exchange the role of $\mathbf{q}_i$ and $\mathbf{q}'_i$ to do so. The problem with this approach is the inconsistency of the epipolar geometry between the two images. To make this more precise, if $\mathbf{F}$ is computed by minimizing $\sum_i d^2(\mathbf{q}'_i, \mathbf{F}\mathbf{q}_i)$ and $\mathbf{F}'$ by minimizing $\sum_i d^2(\mathbf{q}_i, \mathbf{F}'\mathbf{q}'_i)$, there is no warranty that the points of the epipolar line $\mathbf{F}\mathbf{q}$ *different from* $\mathbf{q}'$ correspond to the points of the epipolar line $\mathbf{F}'\mathbf{q}'$. This remark is illustrated by figure 3. The "corresponding" epipolar lines do not correspond at all except on the last column of the grid, where they were defined.

To obtain a consistent epipolar geometry, it is necessary and sufficient that by exchanging the two images, the fundamental matrix is changed to its transpose. This yields the following criterion, which operates simultaneously in the two images:

$$\sum_i (d^2(\mathbf{q}'_i, \mathbf{F}\mathbf{q}_i) + d^2(\mathbf{q}_i, \mathbf{F}^T\mathbf{q}'_i))$$

and can be written, using (14) and the fact that $\mathbf{q}_i'^T\mathbf{F}\mathbf{q}_i = \mathbf{q}_i^T\mathbf{F}^T\mathbf{q}'_i$:

$$\sum_i \left(\frac{1}{(\mathbf{F}\mathbf{q}_i)_1^2 + (\mathbf{F}\mathbf{q}_i)_2^2} + \frac{1}{(\mathbf{F}^T\mathbf{q}'_i)_1^2 + (\mathbf{F}^T\mathbf{q}'_i)_2^2} \right) (\mathbf{q}_i'^T\mathbf{F}\mathbf{q}_i)^2 \qquad (16)$$

This criterion is also clearly normalized in the sense that it does not depend on the scale factor used to compute $\mathbf{F}$.

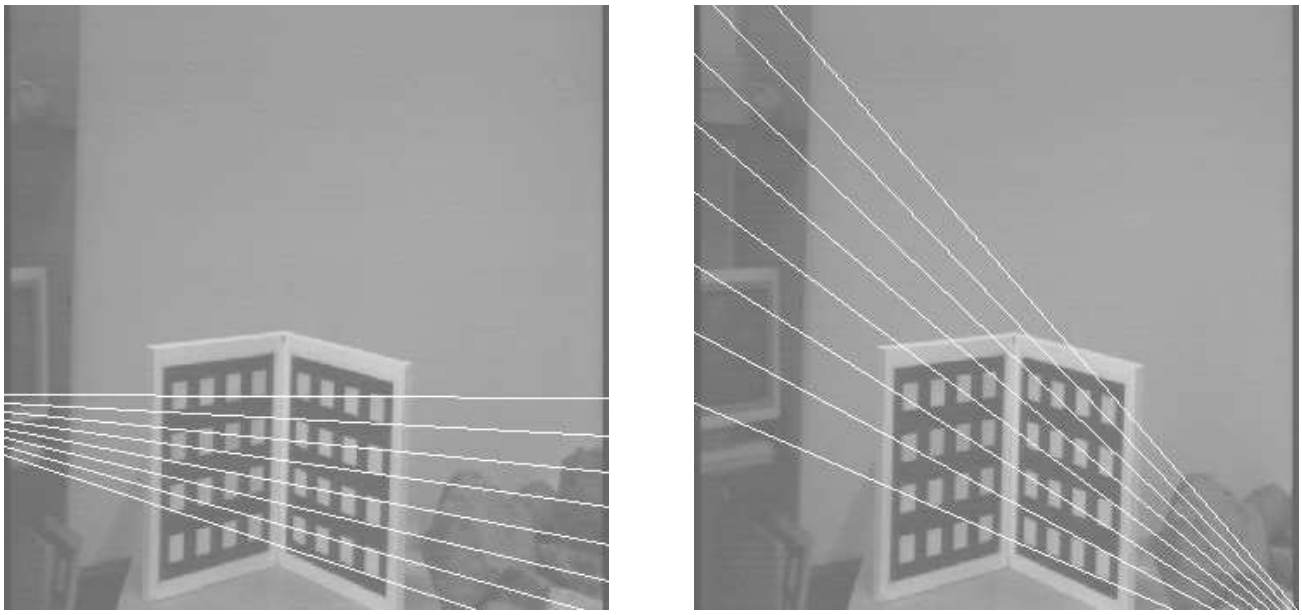

Figure 3: An example of inconsistent epipolar geometry, obtained by independent search in each image

4.2 The Gradient criterion

Taking into account uncertainty Pixels are measured with some uncertainty. When minimizing the expression (9), we have a sum of terms $C_i = \mathbf{q}_i'^T \mathbf{F} \mathbf{q}_i$ which have different variances. It is natural to weight them so that the contribution of each of these terms to the total criterion will be inversely proportional to its variance. The variance of C_i is given as a function of the variance of the points $\mathbf{q}_i$ et $\mathbf{q}_i'$ by:

$$\sigma_{C_i}^2 = \begin{bmatrix} \frac{\partial C_i^T}{\partial \mathbf{q}_i} & \frac{\partial C_i^T}{\partial \mathbf{q}_i'} \end{bmatrix} \begin{bmatrix} \mathbf{\Lambda}_{\mathbf{q}_i} & \mathbf{0} \\ \mathbf{0} & \mathbf{\Lambda}_{\mathbf{q}_i'} \end{bmatrix} \begin{bmatrix} \frac{\partial C_i}{\partial \mathbf{q}_i} \\ \frac{\partial C_i}{\partial \mathbf{q}_i'} \end{bmatrix} \tag{17}$$

where $\Lambda_{\mathbf{q}_i}$ and $\Lambda_{\mathbf{q}_i'}$ are the covariance matrices of the points $\mathbf{q}$ et $\mathbf{q}'$, respectively. These points are uncorrelated as they are measured in different images. We make the classical assumption that their covariance is isotropic and uniform, that is:

$$\Lambda_{\mathbf{q}_i} = \Lambda_{\mathbf{q}_i'} = \begin{bmatrix} \sigma & 0 \\ 0 & \sigma \end{bmatrix}$$

The equation (17) reduces to:

$$\sigma_{C_i}^2 = \sigma^2 \|\nabla C_i\|^2$$

where ∇C_i denotes the gradient of C_i with respect to the four-dimensional vector $(u_i, v_i, u_i', v_i')^T$ built from the affine coordinates of the points $\mathbf{q}_i$ and $\mathbf{q}_i'$. Thus:

$$\nabla C_i = ((\mathbf{F}^T \mathbf{q}_i')_1, (\mathbf{F}^T \mathbf{q}_i')_2, (\mathbf{F} \mathbf{q}_i)_1, (\mathbf{F} \mathbf{q}_i)_2)^T$$

We obtain the following criterion, which is also normalized:

$$\sum_i \frac{(\mathbf{q}_i'^T \mathbf{F} \mathbf{q}_i)^2}{(\mathbf{F}\mathbf{q}_i)_1^2 + (\mathbf{F}\mathbf{q}_i)_2^2 + (\mathbf{F}^T\mathbf{q}_i')_1^2 + (\mathbf{F}^T\mathbf{q}_i')_2^2} \tag{18}$$

We can note that there is a great similarity between this criterion and the distance criterion (16). Each of its terms has the form $\frac{1}{k^2+k'^2}C$, whereas the first one has terms $(\frac{1}{k^2} + \frac{1}{k'^2})C$.

An interpretation as a distance We can also consider the problem of the computing the fundamental matrix from the definition (3) in the general framework of surface fitting, The surface $\mathcal{S}$ is modeled by the implicit equation $g(\mathbf{x}, \mathbf{f}) = 0$, where $\mathbf{f}$ is the sought parameter vector describing the surface which best fits the data points $\mathbf{x}_i$. The goal is to minimize a quantity $\sum_i d(\mathbf{x}_i, \mathcal{S})^2$, where d is a distance. In our case, the data points are the vectors $\mathbf{x}_i = (u_i, v_i, u_i', v_i')$, $\mathbf{f}$ is one of the 7 dimensional parameterizations introduced in the previous section,, and g is given by (3). The linear criterion can be considered as a generalization of the Bookstein distance [1] for conic fitting. The straightforward idea is to approximate the true distance of the point $\mathbf{x}$ to the surface by the number $g(\mathbf{x}, \mathbf{f})$, in order to get a closed-form solution. A more precise approximation has been introduced by Sampson [19]. It is based on the first-order approximation:

$$g(\mathbf{x}) \simeq g(\mathbf{x}_0) + (\mathbf{x} - \mathbf{x}_0) \cdot \nabla g(\mathbf{x}) = g(\mathbf{x}_0) + \|\mathbf{x} - \mathbf{x}_0\| \, \|\nabla g(\mathbf{x})\| \cos(\mathbf{x} - \mathbf{x}_0, \nabla g(\mathbf{x}))$$

If $\mathbf{x}_0$ is the point of $\mathcal{S}$ which is the nearest from $\mathbf{x}$, we have the two properties $g(\mathbf{x}_0) = 0$ and $\cos(\mathbf{x} - \mathbf{x}_0, \nabla g(\mathbf{x}_0)) = 1$. If we make the further first-order approximation that the gradient has the same direction at $\mathbf{x}$ and at $\mathbf{x}_0$: $\cos(\mathbf{x}-\mathbf{x}_0, \nabla g(\mathbf{x}_0)) \simeq \cos(\mathbf{x}-\mathbf{x}_0, \nabla g(\mathbf{x}))$, we get:

$$d(\mathbf{x}, \mathcal{S}) = \|\mathbf{x} - \mathbf{x}_0\| \simeq \frac{g(\mathbf{x})}{\|\nabla g(\mathbf{x})\|}$$

Il is now obvious that the criterion (18) can be written: $\sum_i d(\mathbf{x}_i, \mathcal{S})^2$.

It would be possible to use a second-order approximation such as the one introduced by Nalwa and Pauchon [17], however the experimental results presented in the next section show that it would not be very useful practically. We thus prefer to consider, for theoretical study, the exact distance which is now presented.

4.3 The "Euclidean" criterion

Experience with conic fitting shows that when the data points are not well distributed along the conic on which they lie, the fitting method using the first order approximation of the Euclidean distance of a point to the conic gives results that are somewhat different of those obtained when using a full (i.e. not approximated) Euclidean distance. This is, indeed, what happens with the surface fitting scheme defined in the previous paragraph : the data points are 4-D vectors $\mathbf{x}_i = (u_i, v_i, u_i', v_i')^T$ whose components are image coordinates; since retinas have a finite extent and since the hyper-surface

$\mathcal{S}$ is not bounded [1], the measures of the surface points cover only a small part of the real "underlying" surface. This can also be seen as the following fact : estimating the fundamental matrix is also estimating the epipoles, so it involves the estimation of entities (the epipoles) that are very often far from the image space. Therefore, it seems interesting to develop a criterion based on the Euclidean distance from a 4-D point $\mathbf{x}_i$ to the surface $\mathcal{S}$ in order to check if the results are noticeably different from those obtained when using the gradient criterion.

Fitting a quadratic hyper-surface The hyper-surface $\mathcal{S}$ defined by the equation (3) in the space $\mathcal{R}_1 \times \mathcal{R}_2$ (the cyclopean retina) is quadratic. Moreover, all epipolar lines are on this hyper-surface. Let us note l'_{u_i,v_i} the epipolar line in $\mathcal{R}_2$ corresponding to the point $(u_i, v_i) \in \mathcal{R}_1$ and $l_{u'_i,v'_i}$ the epipolar line in $\mathcal{R}_1$ corresponding to the point $(u'_i, v'_i) \in \mathcal{R}_2$.

The computation of the 4-D Euclidean distance of a point to $\mathcal{S}$ relies on the fact that :

The 4-D lines defined by $u = u_i, v = v_i, (u', v') \in l'_{u_i,v_i}$ and $u' = u'_i, v' = v'_i, (u, v) \in l_{u'_i,v'_i}$ are subsets of $\mathcal{S}$. Thus $\mathcal{S}$ is a ruled surface that can be parametrized by each of these two family of lines[2]. This property is nothing more than writing equation (3) but it gives us these two important parametrizations.

For example, let us parametrize $\mathcal{S}$ using the first family of lines.

Every point of the surface can be represented by $\mathbf{q}_0 = (u_0, v_0)$ and a point of the line $l'_{\mathbf{q}_0} = l'_{u_0,v_0}$, so the distance of a point $(\mathbf{q}, \mathbf{q}') = (u, v, u', v')$ to the surface is given by the minimum of :

$$d^2(\mathbf{q}_0, \mathbf{q}) + d^2(\mathbf{q}', l'_{\mathbf{q}_0})$$

when $\mathbf{q}_0$ describes the space $\mathcal{R}^2$.

Thus the estimation of $\mathbf{F}$ leads to the following minimization :

$$\min_{\mathbf{F}} \sum_i \min_{\mathbf{q}_0} \{d^2(\mathbf{q}_0, \mathbf{q}_i) + d^2(\mathbf{q}'_i, L'_{\mathbf{q}_0})\}$$

As the previous methods, this criterion does no depend on the scale factor applied to $\mathbf{F}$.

5 Parameterizations of the Fundamental Matrix

5.1 A matrix defined up to a scale factor

The most natural idea to take into account the fact that $\mathbf{F}$ is defined only up to a scale factor is to fix one of the coefficients to 1 (only the linear criterion allows us to use in

[1] A point (u_i, v_i) in the first retina $\mathcal{R}_1$ may have its corresponding point that lies at infinity in the second retina $\mathcal{R}_2$

[2] From the point of view of this property the best 3-D analogy is the hyperboloid of one sheet

a simple manner another normalization, namely $\|\mathbf{F}\|$). It yields a parameterization of $\mathbf{F}$ by eight values, which are the ratio of the eight other coefficients to the normalizing one.

In practice, the choice of the normalizing coefficient has significant numerical consequences. As we can see from the expressions of the criteria previously introduced (16) and (18), the non-linear criteria take the general form:

$$\frac{Q_1(F_{11}, F_{12}, F_{13}, F_{21}, F_{22}, F_{23}, F_{31}, F_{32}, F_{33})}{Q_2(F_{11}, F_{12}, F_{13}, F_{21}, F_{22}, F_{23})}$$

where Q_1 and Q_2 are quadratic forms which have null values at the origin. A well-known consequence is that the function Q_1/Q_2 is not regular near the origin. As the derivatives are used in the course of the minimization procedure, this will induce unstability. As a consequence, we have to choose as normalizing coefficients one of the six first one, as only these coefficients appear in the expression of Q_2. Fixing the value of one of these coefficients to one prevents Q_2 from getting near the origin.

We have established using covariance analysis that the choices are not equivalent when the order of magnitude of the different coefficients of $\mathbf{F}$ is different. The best results are theoretically obtained when normalizing with the biggest coefficients. We found in our experiments this observation to be generally true. However, as some cases of divergence during the minimization process sometimes appear, the best is to try several normalizations

We note that as the matrices which are used to initialize the non-linear search are not, in general, singular, we have to compute first the closest singular matrix, and then the parameterization. In that case, we cannot use formulas (6), thus the epipole $\mathbf{e}$ is determined by solving the following classical constrained minimization problem

$$\min_{\mathbf{e}} \|\mathbf{F}\mathbf{e}\|^2 \quad \text{subject to} \quad \|\mathbf{e}\|^2 = 1$$

which yields $\mathbf{e}$ as the unit norm eigenvector of matrix $\mathbf{F}^T\mathbf{F}$ corresponding to the smallest eigenvalue. The same processing applies in reverse to the computation of the epipole e'. The epipolar transformation can then be obtained by a linear least-squares procedure, using equations (5) and (4).

5.2 A singular matrix

As seen in part 3, the drawback of the previous method is that we do not take into account the fact that the rank of $\mathbf{F}$ is only two, and that $\mathbf{F}$ thus depends on only 7 parameters. We have first tried to use minimizations under the constraint $\det(\mathbf{F}) = 0$, which is a cubic polynomial in the coefficients of $\mathbf{F}$. The numerical implementations were not efficient and accurate at all.

Thanks to a suggestion by Luc Robert, we can express the same constraint with an unconstrained minimization: the idea is to write matrix $\mathbf{F}$ as:

$$\mathbf{F} = \begin{pmatrix} a_1 & a_2 & a_3 \\ a_4 & a_5 & a_6 \\ a_7a_1 + a_8a_4 & a_7a_2 + a_8a_5 & a_7a_3 + a_8a_6 \end{pmatrix} \tag{19}$$

The fact that the third line is a linear combination of the two first lines ensures that $\mathbf{F}$ is singular. Chosing such a representation allows us to represent $\mathbf{F}$ by the right number of parameters, once the normalization is done. A non-linear procedure is required, but it is not a drawback, as the criteria presented in section 4 are already non-linear.

5.3 A fundamental matrix with finite epipoles

The previous representation takes into account only the fact that $\mathbf{F}$ is singular. We can use the fact it is a fundamental matrix to parameterize it by the values that are of significance for us. Using the formulas (6) yield:

$$\mathbf{F} = \begin{pmatrix} b & a & -ay - bx \\ -d & -c & cy + dx \\ dy' - bx' & cy' - ax' & -cyy' - dy'x + ayx' + bxx' \end{pmatrix} \tag{20}$$

The parameters that we use are the affine coordinates (x, y) and (x', y') of the two epipoles, and three of the four homography coefficients, which are the coefficients of the submatrix 2×2 obtained by suppressing the third line and the third column. We normalize by the biggest of them. The initial parameters are obtained by computing the epipoles and the epipolar transformation by the approximations introduced in 5.1.

6 An experimental comparison

We have presented an approach to the computation of the fundamental matrix which involves several parameterizations and several criteria. The goal of this part is to provide a statistical comparison of the different combinations.

6.1 The method

An important remark is that if we want to make a precise assessment of the performance of any method, we have to change not only the image noise, as it is often done, but also the displacements. Different displacements will give rise to configurations with stability properties that are very different.

We start from 3D points that are randomly scattered in a cube, and from a projection matrix $\mathbf{P}$. All these values are chosen to be realistic. Each trial consists of:

- Take a random rigid displacement $\mathbf{D}$,
- Compute the exact fundamental matrix $\mathbf{F}_0$ from $\mathbf{D}$ and $\mathbf{P}$,
- Compute the projection matrix $\mathbf{P}'$ from $\mathbf{D}$ and $\mathbf{P}$,
- Project the 3D points in the two 512×512 retinas using $\mathbf{P}$ and $\mathbf{P}'$,
- Add Gaussian noise to the image points,
- Solve for the fundamental matrix $\mathbf{F}$,
- Compute the relative distance of the epipoles from $\mathbf{F}$ and those from $\mathbf{F}_0$.

We measure the error by the relative distance, for each coordinate of the epipole:

$$\min\{\frac{|x - x_0|}{\min(|x|, |x_0|)}, 1\}$$

It should be noted that using relative errors on the coefficients of $\mathbf{F}$, is less appropriate, as the thing we are interested in is actually the correct position of the epipoles. We will also see later that using the value of the minimized criterion as a measure of the error is not appropriate at all: a very coherent epipolar geometry can be observed with completely misplaced epipoles. As our experimentations have shown that the average errors on the four coordinates are always coherent, we will take the mean of these four values as an error measure.

6.2 The linear criteria

We have compared the different implementations of the linear criterion, in the table 6.2. Each entry of the table represents the average relative distance of the results obtained by the two methods represented by the vertical entry and by the horizontal one. The abbreviations are defined in the section on the linear criterion. Conclusions are:

noise		relative distances			
		SVD	**DIAG**	**M-C**	**DIAG-N**
0.2 pixel	**EXACT**	0.1598	0.1543	0.1550	0.1828
	SVD		0.0544	0.0543	0.1511
	DIAG			0.0034	0.1375
	M-C				0.1380
1 pixel	**EXACT**	0.4623	0.4590	0.4590	0.4929
	SVD		0.1077	0.1089	0.3535
	DIAG			0.0040	0.3486
	M-C				0.3488
1.8 pixel	**EXACT**	0.6375	0.6334	0.6336	0.6587
	SVD		0.1442	0.1444	0.4575
	DIAG			0.0055	0.4465
	M-C				0.4465

Table 2: Comparisons of the linear criteria

- The normalization of projective coordinates leads to the worse results
- The two methods **DIAG** and **M-C** are very similar
- The difference between the fist three criterions is not significant, in comparison with the absolute errors, which is normal as the theoretical minimum is unique.

6.3 Non-linear criteria

We have not studied extensively the Euclidean distance criterion, due to the time required for its minimization, which is several hours. However, we have found that it gives results close to, and often more precise than the ones given by the Gradient criterion. There are two different parameterizations, that were presented in section 5, and two different non-linear criteria, presented in section 4. The abbreviations for the four resulting combinations that we studied are in table 3. We have tried several minimization procedures, including material from Numerical Recipes, and programs from the NAG library.

Table 3: Non-linear methods for the computation of the fundamental matrix

abbrev.	criterion	parameterization
LIN	linear	normalization by $\|\mathbf{F}\|$
DIST-L	distance to epipolar lines 16	singular matrix 19
DIST-T	distance to epipolar lines	epipolar transformation 20
GRAD-L	weighting by the gradient 18	singular matrix
GRAD-T	weighting by the gradient	epipolar transformation

The comparison we have done is threefold:

1. *The stability of the minimum corresponding to the exact solution.* When noise is present, the surface which represents the value of the criterion as a function of the parameters gets distorted, thus the coordinates of the minimum change. A measure of this variation is given by the distance between the exact epipole and the one obtained when starting the minimization with the exact epipole (figure 4).
2. *The convergence properties.* The question is whether it is possible to obtain a correct result starting from a plausible initialization, the matrix obtained from the linear criterion. We thus measure the distance between the exact epipole and the one obtained when starting the minimization with the linear solution (figure 5), and the distance between the epipole obtained when starting the minimization with the exact epipole and the one obtained when starting the minimization with the linear solution (figure 6) .
3. *The stability of the criterion.* When the surface which represents the value of the criterion as a function of the parameters gets distorted, the values of the criterion at local minima corresponding to inexact solutions can become weaker than the value of the criterion at the correct minimum (figure 7).

The conclusions are:

- *The non-linear criteria are always better than the linear criterion.* When starting a non-linear computation with the result of the linear computation, we always improve the precision of the result, even if the noise is not important. The difference increases with the noise.

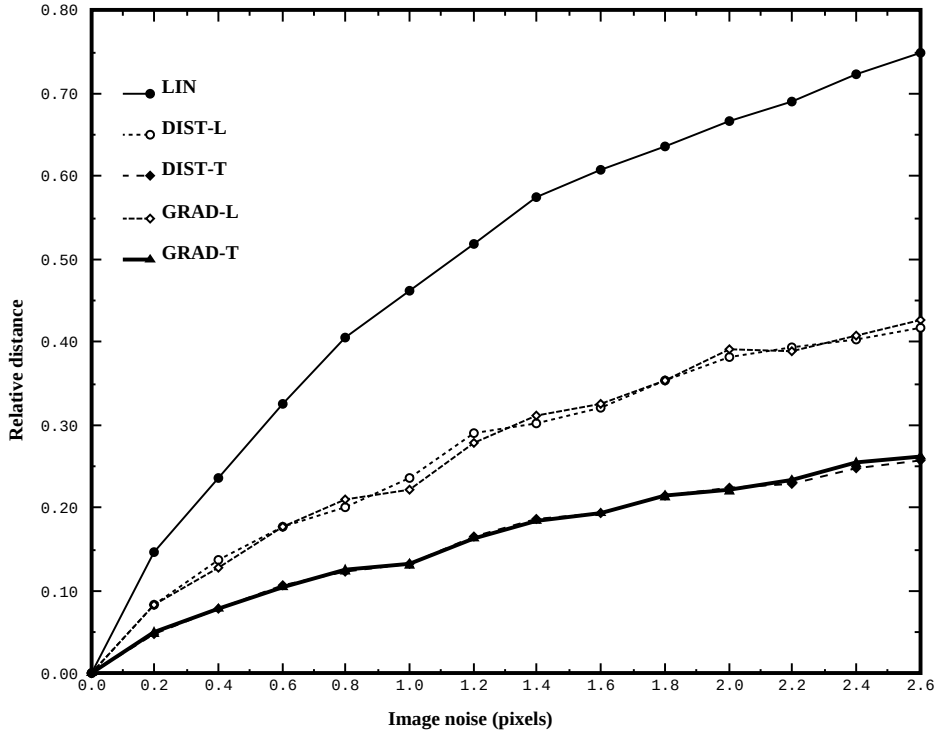

Figure 4: Relative distances obtained starting from the exact values

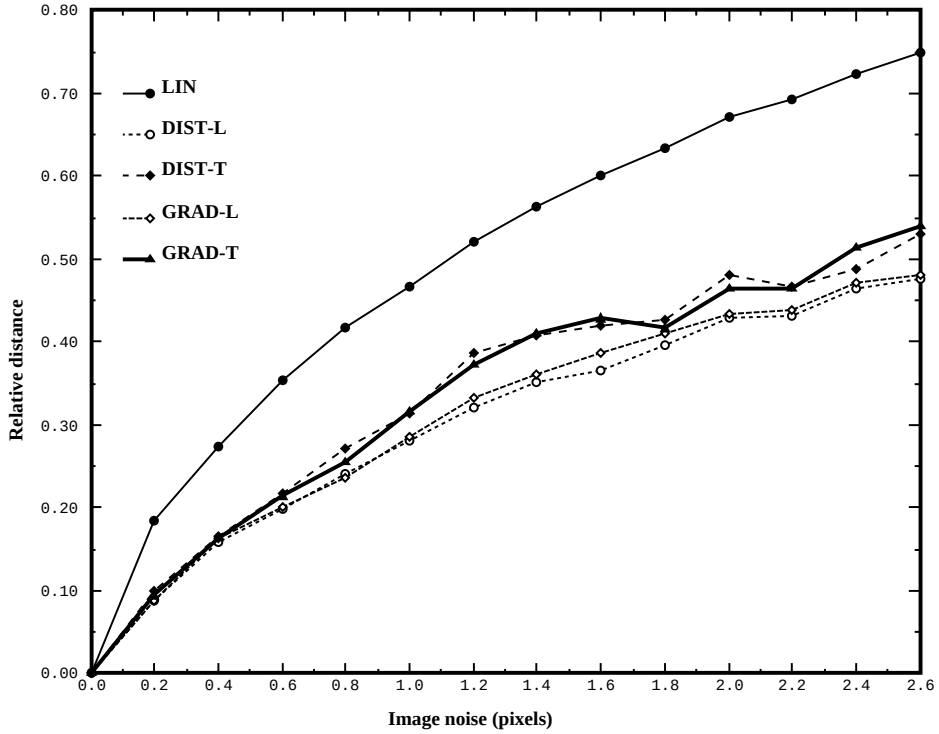

Figure 5: Relative distances obtained starting from the values found by the linear criterion

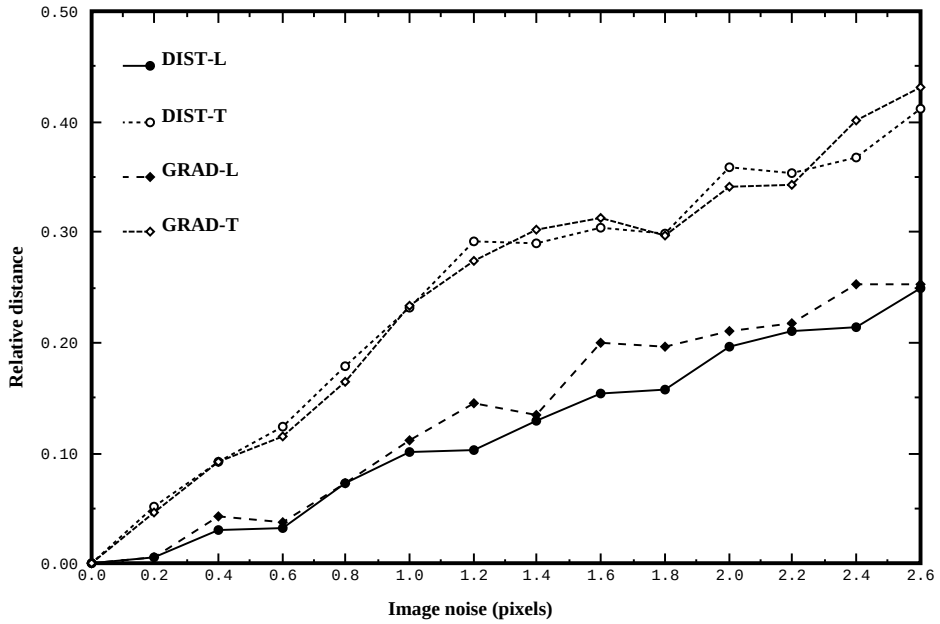

Figure 6: Relative distances obtained between results of the two different initializations

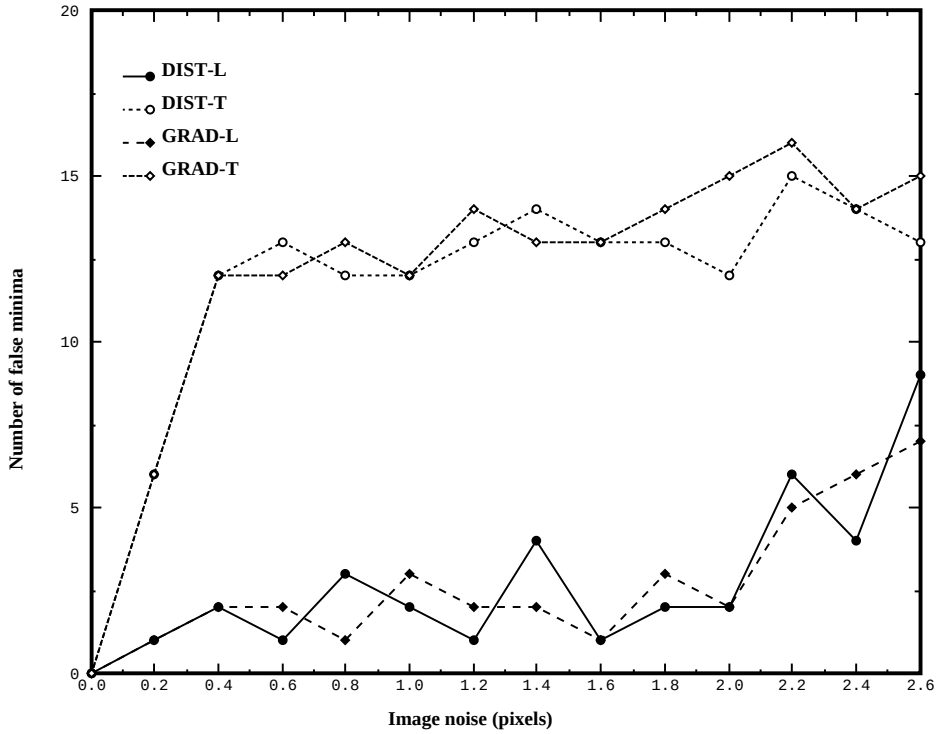

Figure 7: Number of false minima

- The difference due to the choice of the criterion (**DIST** or **GRAD**) is much less significant than the one due to the choice of the parameterization (**L** or **T**).
- The parameterization **T** yields more stable minima than the parameterization **L**, as seen in figure 4.
- However, the criterion obtained with parameterization **T** has worse convergence and stability properties than the parameterization **L** , as seen in figures 6 and 7
- As a consequence, when starting from the results of the linear criterion, the results of the four non-linear combinations are roughly equivalent, the results obtained with the parameterization **L** and the criterion **DIST** being slightly better, as seen in figure 5.
- The computation is quite sensitive to pixel noise: a Gaussian noise of variance 1 pixel yields a relative error which is about 30%.

6.4 Real data

We now illustrate the remarks made in section 3 with a pair of images. It can be seen in figure 8 that the pencils of epipolar lines obtained with the linear criterion, and those obtained with the non-linear criterion are very different. The epipoles obtained with the non-linear criterion are much further away. It seems at first that if one considers a point that was used in the computation, its epipolar line lies very close to its corresponding point. However, the zoom of figure 9 shows that the fit is significantly better with the non-linear criterion. Figure 10 shows a set of epipolar lines obtained from the linear criterion, we can see that they don't meet exactly at a point, whereas they do by construction for the non-linear criterion. A consequence is illustrated in figure 11, which shows some more epipolar lines, drawn from points that were *not* used in the computation of the fundamental matrix. It can be seen that for the points on the wall, which are quite far from the epipole, the corresponding epipolar lines seem approximately correct, while for the points chosen on the table, the corresponding epipolar lines are obviously very incorrect, in the sense they are very far from the corresponding points. This situation does not occur with the non-linear criterion, as it can be seen in the bottom of this figure.

7 Conclusion

In this paper, we focused on the problem of determining in a robust way the *Fundamental matrix* from a given number of image point correspondences. Its properties and relations to the well-known *Essential matrix* have been made very clear. Different parametrizations for this matrix have been proposed and a large number of criteria have been considered and analyzed in great detail to tackle efficiently this problem. The classical linear criterion has been shown to be unable to express the rank and normalization constraints, and different non-linear criteria have been proposed to overcome its major weaknesses. It has been shown that the use of non-linear criteria leads to the best results and an extensive experimental work on noisy synthetic data and real

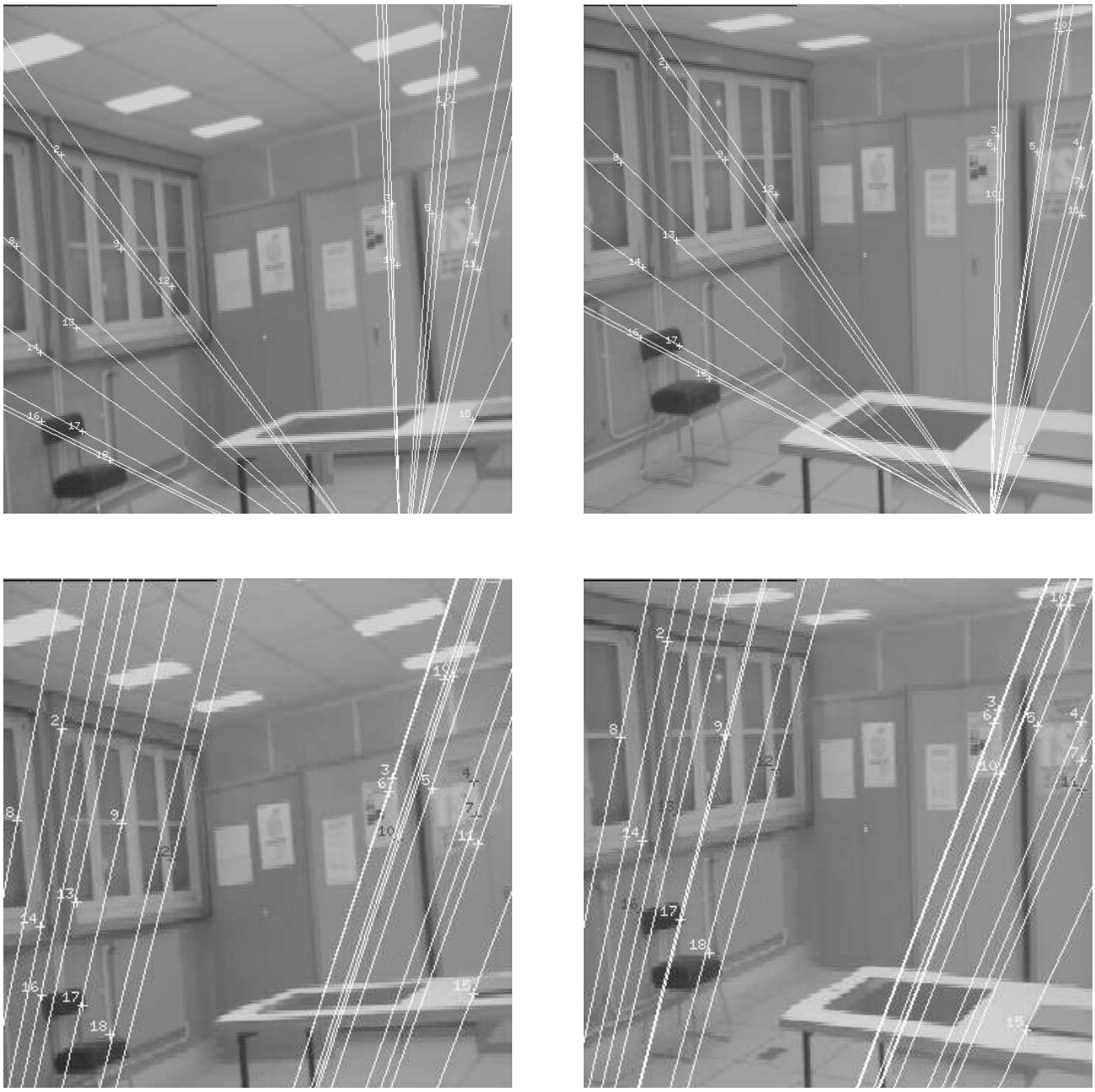

Figure 8: Epipolar lines obtained from the linear criterion (top), and from the non-linear criterion (bottom)

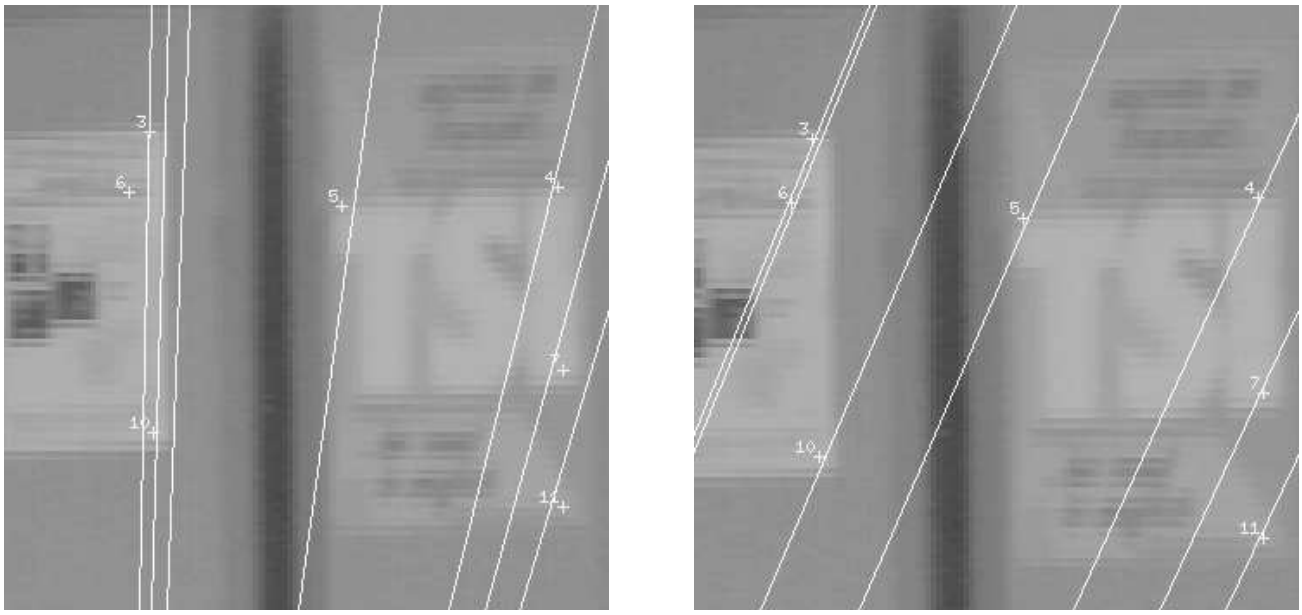

Figure 9: Zoom showing the fit with the linear criterion (left) and the non-linear criterion (right)

images has been carried out to evaluate stability and convergence properties of each method.

References

[1] F. L. Bookstein. Fitting conic sections to scattered data. *Computer Graphics and Image Processing*, 9(1):56–71, Jan 1979.

[2] J.Q. Fang and T.S. Huang. Some experiments on estimating the 3D motion parameters of a rigid body from two consecutive image frames. *IEEE Transactions on Pattern Analysis and Machine Intelligence*, 6:545–554, 1984.

[3] O.D. Faugeras. What can be seen in three dimensions with an uncalibrated stereo rig. In *Proc. European Conference on Computer Vision*, pages 563–578, 1992.

[4] O.D. Faugeras, Q.-T. Luong, and S.J. Maybank. Camera self-calibration: theory and experiments. In *Proc. European Conference on Computer Vision*, pages 321–334, 1992.

[5] O.D. Faugeras and G. Toscani. The calibration problem for stereo. In *Proceedings of CVPR'86*, pages 15–20, 1986.

[6] R.I. Hartley. Estimation of relative camera positions for uncalibrated cameras. In *Proc. European Conference on Computer Vision*, pages 579–587, 1992.

[7] T.S. Huang and O.D. Faugeras. Some properties of the E-matrix in two view motion estimation. *IEEE Transactions on Pattern Analysis and Machine Intelligence*, 11:1310–1312, 1989.

[8] Koenderink J. J. and A. J. van Doorn. Affine Structure from Motion. *Journal of the Optical Society of America A*, 8(2):377–385, 1992.

[9] D.G. Jones and J. Malik. A Computational Framework for Determining Stereo Correspondence from a Set of Linear Spatial Filters. In *Proc. European Conference on Computer Vision*, pages 395–410, 1992.

[10] K. Kanatani. Computational projective geometry. *Computer Vision, Graphics, and Image Processing. Image Understanding*, 54(3), 1991.

[11] C.H. Lee. Time-varying images: the effect of finite resolution on uniqueness. *Computer Vision, Graphics, and Image Processing. Image Understanding*, 54(3):325–332, 1991.

[12] C. Longuet-Higgins. The reconstruction of a scene from two projections: configurations that defeat the 8-point algorithm. In *Proc. 1st Conf. on Artificial intelligence applications*, pages 395–397, Denver, 1984.

[13] H.C. Longuet-Higgins. A Computer Algorithm for Reconstructing a Scene from Two Projections. *Nature*, 293:133–135, 1981.

[14] S.J. Maybank and O.D. Faugeras. A Theory of Self-Calibration of a Moving Camera. *The International Journal of Computer Vision*, 8(2):123–151, 1992.

[15] R. Mohr, L. Quan, F. Veillon, and B. Boufama. Relative 3d reconstruction using multiple uncalibrated images. Technical Report RT84-IMAG12, LIFIA, June 1992.

[16] J. L. Mundy and A. Zisserman, editors. *Geometric invariance in computer vision.* MIT Press, 1992.

[17] V.S. Nalwa and E. Pauchon. Edgel aggregation and edge description. *Computer Vision, Graphics, and Image Processing*, 40(1):79–94, Oct. 1987.

[18] S.I. Olsen. Epipolar line estimation. In *Proc. European Conference on Computer Vision*, pages 307–311, 1992.

[19] P.D. Sampson. Fitting conic sections to very scattered data. an iterative refinement of the Bookstein algorithm. *Computer Graphics and Image Processing*, 18(1):97–108, Jan. 1982.

[20] A. Shashua. Projective structure from two uncalibrated images: structure from motion and recognition. Technical Report A.I. Memo No. 1363, MIT, Sept 1992.

[21] R.Y. Tsai. An Efficient and Accurate Camera Calibration Technique for 3D Machine Vision. In *Proceedings CVPR '86, Miami Beach, Florida*, pages 364–374. IEEE, June 1986.

[22] R.Y. Tsai and T.S. Huang. Uniqueness and estimation of three-dimensional motion parameters of rigid objects wirth curved surfaces. *IEEE Transactions on Pattern Analysis and Machine Intelligence*, 6:13–27, 1984.

[23] J. Weng, T.S. Huang, and N. Ahuja. Motion and structure from two perspective views: algorithms, error analysis and error estimation. *IEEE Transactions on Pattern Analysis and Machine Intelligence*, 11(5):451–476, 1989.

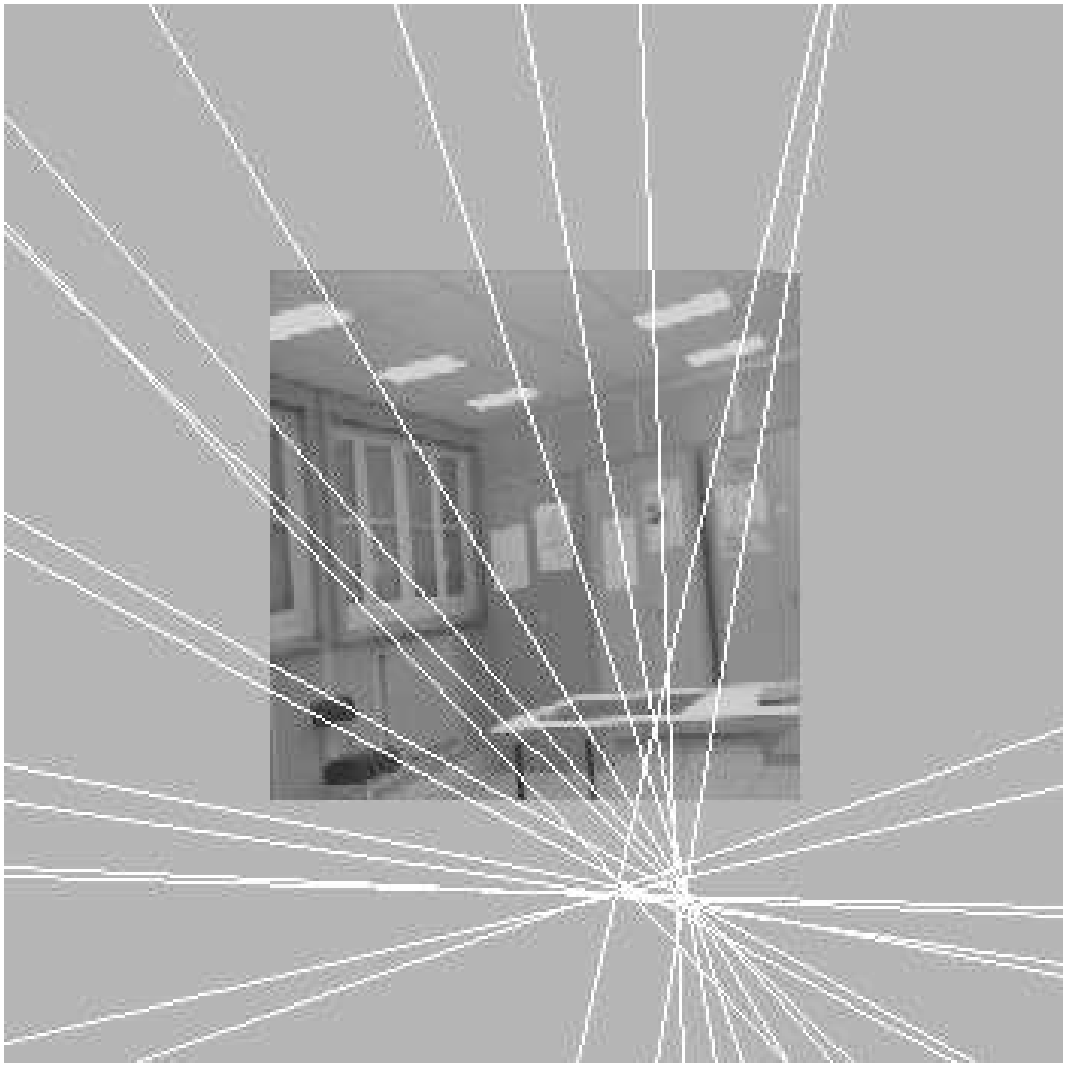

Figure 10: Intersection of epipolar lines obtained from the linear criterion

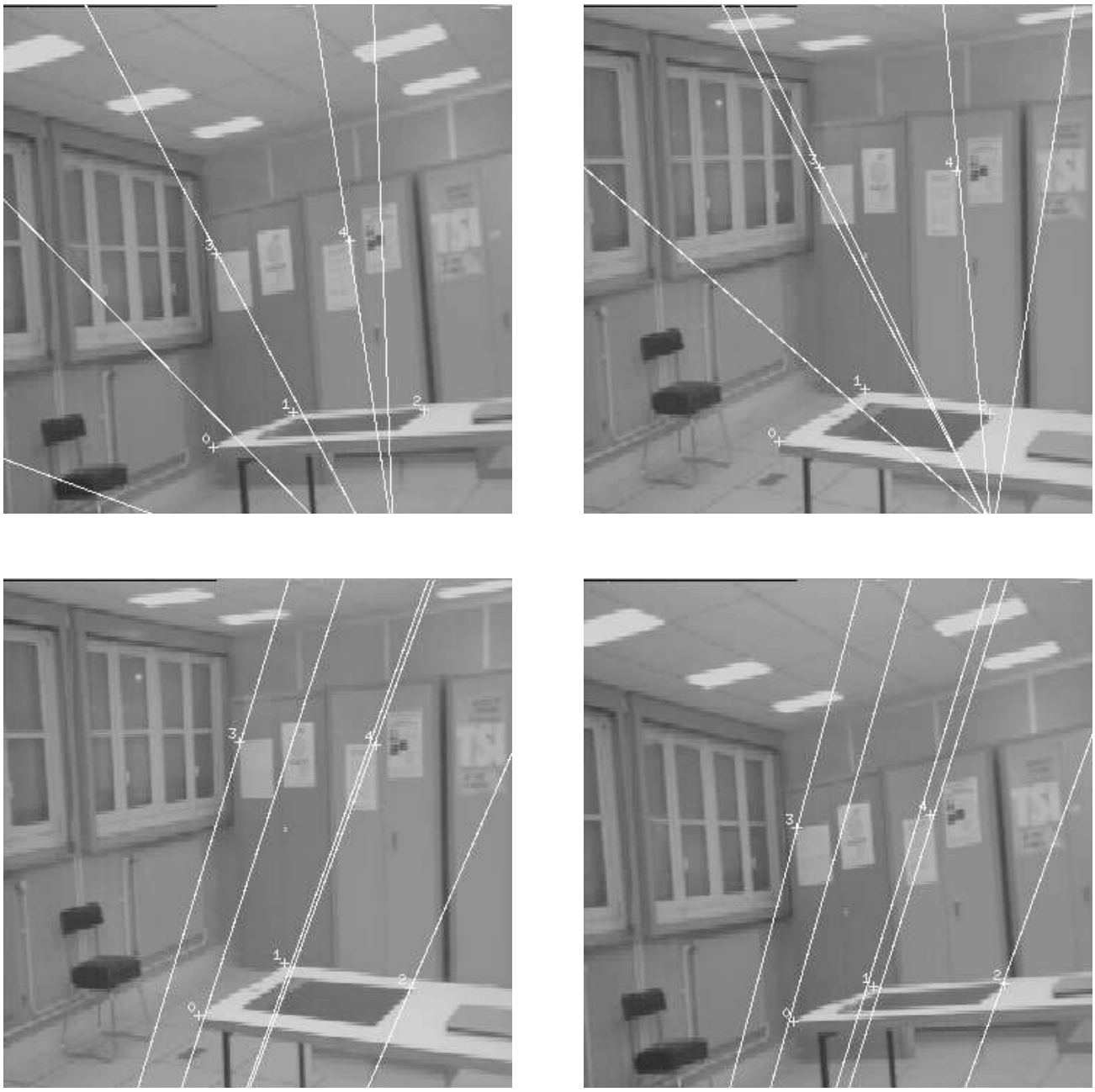

Figure 11: Additional epipolar lines obtained with the linear criterion (top), and with the non-linear criterion (bottom)